Earth Syst. Dynam. Discuss., https://doi.org/10.5194/esd-2018-88
Manuscript under review for journal Earth Syst. Dynam.
Discussion started: 17 December 2018

Earth System Dynamics Discussions
Open Access
EGU

Including the efficacy of land ice changes in deriving climate sensitivity from paleodata

Lennert B. Stap[1], Peter Köhler[1], and Gerrit Lohmann[1]

[1]Alfred-Wegener-Institut, Helmholtz-Zentrum für Polar- und Meeresforschung, Am Handelshafen 12, 27570 Bremerhaven, Germany

Correspondence: L.B. Stap (lennert.stap@awi.de)

Abstract. The influence of long-term processes in the climate system, such as land ice changes, has to be compensated for when comparing climate sensitivity derived from paleodata with equilibrium climate sensitivity (ECS) calculated by climate models, which is only generated by a CO_2 change. Several recent studies found that the impact these long-term processes have on global temperature cannot be quantified directly through the global radiative forcing they induce. This renders the approach of deconvoluting paleotemperatures through a partitioning based on radiative forcings inaccurate. Here, we therefore implement an efficacy factor $\varepsilon_{[LI]}$, that relates the impact of land ice changes on global temperature to that of CO_2 changes, in our calculation of climate sensitivity from paleodata. We apply our new approach to a proxy-inferred paleoclimate dataset, and find an equivalent ECS of $5.6 \pm 1.3\,K$ per CO_2 doubling. The substantial uncertainty herein is generated by the range in $\varepsilon_{[LI]}$ we use, which is based on a multi-model assemblage of simulated relative influences of land ice changes on the Last Glacial Maximum (LGM) temperature anomaly ($46 \pm 14\%$). The low end of our ECS estimate, which concurs with estimates from other approaches, tallies with a large influence for land ice changes. To separately assess this influence, we analyse output of the PMIP3 climate model intercomparison project. From this data, we infer a functional intermodel relation between global and high-latitude temperature changes at the LGM with respect to the pre-industrial climate, and the temperature anomaly caused by a CO_2 change. Applying this relation to our dataset, we find a considerable 64% influence for land ice changes on the LGM temperature anomaly. This is even higher than the range used before, and leads to an equivalent ECS of 3.8 K per CO_2 doubling. Together, our results suggest that land ice changes play a key role in the variability of Late Pleistocene temperatures.

Earth Syst. Dynam. Discuss., https://doi.org/10.5194/esd-2018-88
Manuscript under review for journal Earth Syst. Dynam.
Discussion started: 17 December 2018

Earth System Dynamics Discussions

1 Introduction

Equilibrium climate sensitivity (ECS) expresses the simulated equilibrated surface air temperature response to an instantaneous CO_2 doubling. The simulated effect of the applied CO_2 radiative forcing anomaly includes the Planck response, as well as the fast feedbacks e.g. through snow, sea ice, lapse rate, clouds and water vapour changes. ECS varies significantly between different state-of-the-art climate models, as for instance the CMIP5 ensemble shows a range of 1.9 to 4.4 K (Vial et al., 2013). Several ways have been put forward to constrain ECS, for example through the usage of paleoclimate data (e.g. Covey et al., 1996; Edwards et al., 2007), which is also the focus of this study. However, unlike results of models, which can be run ceteris paribus, temperature reconstructions based on paleoclimate proxy data always contain a mixed signal of all processes active in the climate system. Among these are long-term processes (or slow feedbacks) such as changes in vegetation, dust, and, arguably most importantly, land ice changes, which are not taken into account in the quantification of ECS. Therefore, it is necessary to correct paleotemperature records for the influence of these processes, in order to make a meaningful comparison to ECS calculated by climate models.

In a co-ordinated community effort, the PALAEOSENS project proposed to relate the temperature response caused by these long-term processes to the global averaged radiative forcing they induce (PALAEOSENS Project Members, 2012). Consequently, the paleotemperature record can be disentangled on the basis of the separate radiative forcings of these long-term processes (e.g. von der Heydt et al., 2014; Martínez-Botí et al., 2015; Köhler et al., 2015, 2017b, 2018; Friedrich et al., 2016). If all processes are accounted for in this manner, the sole effect of CO_2 changes, as is asserted by the ECS, can be quantified. However, several studies have shown that, depending on the type of radiative forcing, the same global average radiative forcing can lead to different global temperature changes (e.g. Stuber et al., 2005; Hansen et al., 2005; Yoshimori et al., 2011). For instance, in a previous article (Stap et al., 2018) we simulated the separate and combined effects of CO_2 changes and land ice changes on global surface air temperature using the intermediate complexity climate model CLIMBER-2 and showed that the specific global temperature change per unit radiative forcing change depends on which process is involved. As a possible solution to this problem, Hansen et al. (2005) formulated the concept of 'efficacy' factors, which express the impact of radiative forcing by a certain process in comparison to the effect of radiative forcing by CO_2 changes.

In this study, we use this concept of efficacy from Hansen et al. (2005) to refine a previous estimate of climate sensitivity based on a paleoclimate dataset of the past 800 kyr (Köhler et al., 2015, 2018). Before pursuing this, we demonstrate the inclusion of a constant efficacy factor for radiative forcing by albedo changes due to land ice variability on transient simulations over the past 5 Myr using CLIMBER-2. In the results of these simulations, the separate and combined effects of the greenhouse gas radiative forcing of CO_2 and of the radiative forcing caused by land ice changes are obtained from different model setups (Stap et al., 2018). In the analysis of the paleoclimate dataset of Köhler et al. (2015), we appraise the influence of land ice changes and the associated efficacy in two manners, because here it is not a-priori known. Firstly, we use a range that is given by different modelling efforts of the Last Glacial Maximum (LGM; $\sim$20 kyr ago) (Shakun, 2017). The climate sensitivity resulting from applying this range provides a quantification of the consequence of the uncertain efficacy of land ice changes.

Earth Syst. Dynam. Discuss., https://doi.org/10.5194/esd-2018-88
Manuscript under review for journal Earth Syst. Dynam.
Discussion started: 17 December 2018

Earth System Dynamics Discussions Open Access EGU

Secondly, we analyse data from the PMIP3 climate model intercomparison LGM experiment (Braconnot et al., 2012) to find a separate estimate of this efficacy in our dataset, along with the accessory climate sensitivity.

2 Material and methods

2.1 Approach

Equilibrium climate sensitivity (ECS) is the global average surface air temperature change resulting from a CO_2 doubling ($\Delta T_{[CO_2]}$), and is usually obtained from climate model simulations. In these simulations, fast feedbacks, i.e. processes in the climate system with timescales of less than ∼100 yrs, are accounted for. However, slower processes, such as ice sheet, vegetation and dust changes, are commonly kept constant. The resulting response is also sometimes called 'Charney' sensitivity (Charney et al., 1979). Recently, it has been shown that simulations of models that have been integrated over a few centuries are not yet in equilibrium, and from longer climate simulations a higher ECS can be deduced (Knutti et al., 2017). Another way to express equilibrium climate sensitivity, is by taking the ratio of the temperature change over the radiative forcing due to the CO_2 change ($\Delta R_{[CO_2]}$), leading to S^a (where a stands for *actuo*) following the notation of PALAEOSENS Project Members (2012):

$$S^a = \frac{\Delta T_{[CO_2]}}{\Delta R_{[CO_2]}}. \tag{1}$$

The subscript denotes that CO_2 is the only long-term process involved. Analogously, paleoclimate sensitivity (S^p) can be deduced from paleo-temperature reconstructions and paleo-CO_2 records as

$$S^p = \frac{\Delta T_g}{\Delta R_{[CO_2]}}. \tag{2}$$

In this case, the global paleotemperature anomaly with respect to the pre-industrial (PI) average (ΔT_g) is, however, also affected by the long-term processes that are typically neglected in the climate simulations. Therefore, a correction to the paleotemperature perturbation is needed to obtain $\Delta T_{[CO_2]}$ from ΔT_g:

$$\Delta T_{[CO_2]} = \Delta T_g (1 - f), \tag{3}$$

or equivalently S^a from S^p:

$$S^a = S^p (1 - f) = \frac{\Delta T_g}{\Delta R_{[CO_2]}} (1 - f). \tag{4}$$

Here, f represents the effect of the slow feedbacks on paleotemperature (e.g. van de Wal et al., 2011). To obtain f, PALAEOSENS Project Members (2012) proposed an approach, which has subsequently been used in numerous studies aiming to constrain climate sensitivity from paleodata (e.g. von der Heydt et al., 2014; Martínez-Botí et al., 2015; Köhler et al., 2015, 2017b, 2018; Friedrich et al., 2016). They suggested to quantify the influence of the long-term processes (X) by the radiative forcing change they induce ($\Delta R_{[X]}$), relative to the total radiative forcing perturbation:

$$f = \frac{\Delta R_{[X]}}{\Delta R_{[CO_2]} + \Delta R_{[X]}} = 1 - \frac{\Delta R_{[CO_2]}}{\Delta R_{[CO_2]} + \Delta R_{[X]}} \tag{5}$$

Earth Syst. Dynam. Discuss., https://doi.org/10.5194/esd-2018-88
Manuscript under review for journal Earth Syst. Dynam.
Discussion started: 17 December 2018

Earth System Dynamics Discussions

Combining Eqs. 4 and 5 and following the PALAEOSENS nomenclature, we can then derive the 'specific' paleoclimate sensitivity $S_{[CO_2,X]}$, where X represents the processes that are accounted for in the calculation of f:

$$S_{[CO_2,X]} = \frac{\Delta T_g}{\Delta R_{[CO_2]}}\left(1 - \frac{\Delta R_{[X]}}{\Delta R_{[CO_2]} + \Delta R_{[X]}}\right) = \frac{\Delta T_g}{\Delta R_{[CO_2]} + \Delta R_{[X]}} = \frac{\Delta T_g}{\Delta R_{[CO_2,X]}}. \quad (6)$$

If, for instance, the calculated specific paleoclimate sensitivity is only corrected for the most important slow feedback in the climate system, namely radiative forcing anomalies induced by albedo changes due to land ice (LI) variability, one derives:

$$S_{[CO_2,LI]} = \frac{\Delta T_g}{\Delta R_{[CO_2]} + \Delta R_{[LI]}} = \frac{\Delta T_g}{\Delta R_{[CO_2,LI]}}. \quad (7)$$

An overview of different values of $S_{[CO_2,LI]}$ for both colder- and warmer-than-present climates has been compiled by von der Heydt et al. (2016). Using this approach, several studies performed a least-squares regression through scattered data from paleotemperature and radiative forcing records (Martínez-Botí et al., 2015; Friedrich et al., 2016; Köhler et al., 2015, 2017b, 2018) relating ΔT_g to $\Delta R_{[CO_2,LI]}$ in a time-independent manner, from which $S_{[CO_2,LI]}$ could be determined. In this way, a state dependency of $S_{[CO_2,LI]}$ as function of background climate has been deduced for those data which are best approximated by a non-linear function. Furthermore, the quantification of $S_{[CO_2,LI]}$ for those state-dependent cases has been formalized in Köhler et al. (2017b).

The validity of the PALAEOSENS approach to calculate f is contingent on the notion that equal global-average radiative forcing changes lead to equal global temperature responses, regardless of the processes involved. However, it has been demonstrated that the horizontal and vertical distribution of the radiative forcing affects the resulting temperature response (e.g. Stuber et al., 2005; Hansen et al., 2005; Yoshimori et al., 2011; Stap et al., 2018), e.g. because different fast feedbacks are triggered depending on the location of the forcing. To address this issue, Hansen et al. (2005) introduced the concept of 'efficacy' factors, which we will explore further in this study. They related the temperature response to radiative forcing caused by processes X to that caused by CO_2 changes, through efficacy factors ($\varepsilon_{[X]}$), which demands a reformulation of f as f_ε:

$$f_\varepsilon = \frac{\varepsilon_{[X]}\Delta R_{[X]}}{\Delta R_{[CO_2]} + \varepsilon_{[X]}\Delta R_{[X]}} = 1 - \frac{\Delta R_{[CO_2]}}{\Delta R_{[CO_2]} + \varepsilon_{[X]}\Delta R_{[X]}}, \quad (8)$$

and hence also of $S_{[CO_2,X]}$ as $S^{\varepsilon}_{[CO_2,X]}$:

$$S^{\varepsilon}_{[CO_2,X]} = \frac{\Delta T_g}{\Delta R_{[CO_2]} + \varepsilon_{[X]}\Delta R_{[X]}}. \quad (9)$$

In these reformulations, where in principal $\varepsilon_{[X]}$ can take any value, we introduce the superscript ε to clearly distinguish them from the former ones of the PALAEOSENS project, in which the radiative forcing of the different processes had identical weights.

In the following, likewise as several earlier studies (e.g. von der Heydt et al., 2014; Martínez-Botí et al., 2015; Köhler et al., 2015, 2017b, 2018) we focus on the calculation of $S^{\varepsilon}_{[CO_2,LI]}$. To this end, we constrain the efficacy factor for radiative forcing by land ice changes ($\varepsilon_{[LI]}$), using a slightly different definition than Hansen et al. (2005):

$$\frac{\Delta T_{[LI]}}{\Delta R_{[LI]}} = \varepsilon_{[LI]}\frac{\Delta T_g - \Delta T_{[LI]}}{\Delta R_{[CO_2]}}. \quad (10)$$

Earth Syst. Dynam. Discuss., https://doi.org/10.5194/esd-2018-88
Manuscript under review for journal Earth Syst. Dynam.
Discussion started: 17 December 2018

This leads to:

$$\varepsilon_{[\mathrm{LI}]} = \frac{\omega}{1-\omega}\frac{\Delta R_{[\mathrm{CO_2}]}}{\Delta R_{[\mathrm{LI}]}}, \tag{11}$$

where ω represents the fractional relative influence of land ice changes on the global temperature change ($\omega = \Delta T_{[\mathrm{LI}]}/\Delta T_{\mathrm{g}}$). If $\varepsilon_{[\mathrm{LI}]}$ is assumed to be constant in time (see Sect. 3.1 and 4), it can be calculated using Eq. 11 from data covering any moment in time, for instance the Last Glacial Maximum (LGM), and consequently applied to the whole record of $\Delta R_{[\mathrm{CO_2}]}$ and $\Delta R_{[\mathrm{LI}]}$. Similarly as in the old approach, with this $\varepsilon_{[\mathrm{LI}]}$ a quantification of $S^{\varepsilon}_{[\mathrm{CO_2,LI}]}$ can be obtained by performing a least-squares regression through scattered data from paleotemperature and radiative forcing records, now relating ΔT_{g} to $(\Delta R_{[\mathrm{CO_2}]} + \varepsilon_{[\mathrm{LI}]}\Delta R_{[\mathrm{LI}]})$ in a time-independent manner. However, here we take a further simplifying step, which enables one to more readily compare $S^{\varepsilon}_{[\mathrm{CO_2,LI}]}$ to other specific paleoclimate sensitivities $S^{\varepsilon}_{[\mathrm{CO_2,X}]}$ by unifying the dependent variable. We consider:

$$S^{\varepsilon}_{[\mathrm{CO_2,LI}]} = \frac{\Delta T_{\mathrm{g}}}{\Delta R_{[\mathrm{CO_2}]} + \varepsilon_{[\mathrm{LI}]}\Delta R_{[\mathrm{LI}]}} = \frac{\Delta T_{\mathrm{g}}}{\Delta R_{[\mathrm{CO_2}]}}\frac{\Delta R_{[\mathrm{CO_2}]}}{\Delta R_{[\mathrm{CO_2}]} + \varepsilon_{[\mathrm{LI}]}\Delta R_{[\mathrm{LI}]}} = \frac{\Delta T^{\varepsilon}_{[\mathrm{CO_2-equiv}]}}{\Delta R_{[\mathrm{CO_2}]}}. \tag{12}$$

Here, the $\mathrm{CO_2}$-equivalent temperature change ($\Delta T^{\varepsilon}_{[\mathrm{CO_2-equiv}]}$) is defined as:

$$\Delta T^{\varepsilon}_{[\mathrm{CO_2-equiv}]} := \Delta T_{\mathrm{g}}\frac{\Delta R_{[\mathrm{CO_2}]}}{\Delta R_{[\mathrm{CO_2}]} + \varepsilon_{[\mathrm{LI}]}\Delta R_{[\mathrm{LI}]}}. \tag{13}$$

The superscript ε in $\Delta T^{\varepsilon}_{[\mathrm{CO_2-equiv}]}$ is intended to remind us that the efficacy of different radiative forcing is taken into account.

A functional relationship between $\Delta T^{\varepsilon}_{[\mathrm{CO_2-equiv}]}$ and $\Delta R_{[\mathrm{CO_2}]}$ ($\Delta T^{\varepsilon}_{[\mathrm{CO_2-equiv}]} = g(\Delta R_{[\mathrm{CO_2}]})$) can be obtained by least-squares regressions of higher-order polynomial to the scattered data of these variables. We use the precondition that no change in $\mathrm{CO_2}$ is related to no change in $\Delta T^{\varepsilon}_{[\mathrm{CO_2-equiv}]}$, meaning the regression intersects the y-axis at the origin ($(x,y) = (0,0)$). Following Köhler et al. (2017b), for any non-zero $\Delta R_{[\mathrm{CO_2}]}$, $S^{\varepsilon}_{[\mathrm{CO_2,LI}]}$ follows from:

$$S^{\varepsilon}_{[\mathrm{CO_2,LI}]} = \frac{g(\Delta R_{[\mathrm{CO_2}]})}{\Delta R_{[\mathrm{CO_2}]}}. \tag{14}$$

If $\Delta R_{[\mathrm{CO_2}]} = 0\,\mathrm{W\,m^{-2}}$, as is among others the case for pre-industrial conditions, $S^{\varepsilon}_{[\mathrm{CO_2,LI}]}$ is quantified as:

$$S^{\varepsilon}_{[\mathrm{CO_2,LI}]}\Big|_{\Delta R_{[\mathrm{CO_2}]}=0} = \frac{\delta(g)}{\delta(\Delta R_{[\mathrm{CO_2}]})}\Big|_{\Delta R_{[\mathrm{CO_2}]}=0}. \tag{15}$$

Equations 14 and 15 yield a quantification of $S^{\varepsilon}_{[\mathrm{CO_2,LI}]}$, which can be compared to the value obtained for $S_{[\mathrm{CO_2,LI}]}$ using the old approach (Köhler et al., 2018).

2.2 Datasets

2.2.1 CLIMBER-2 model simulations

To demonstrate our approach, we apply it to simulations over the past 5 Myr, which were performed using the intermediate complexity climate model CLIMBER-2 (Petoukhov et al., 2000; Ganopolski et al., 2001). CLIMBER-2 combines a 2.5

Earth Syst. Dynam. Discuss., https://doi.org/10.5194/esd-2018-88
Manuscript under review for journal Earth Syst. Dynam.
Discussion started: 17 December 2018

statistical-dynamical atmosphere model, with a 3-basin zonally averaged ocean model (Stocker et al., 1992), and a model that calculates dynamic vegetation cover based on the temperature and precipitation (Brovkin et al., 1997). The simulations were extensively described in Stap et al. (2018). In brief, they are forced by solar insolation which changes due to orbital (O) variations (Laskar et al., 2004), and further by land ice (I) changes on both hemispheres (based on de Boer et al., 2013), and CO_2 (C) changes (based on van de Wal et al., 2011). In the reference experiment (OIC) all input data are varied, while in other model integrations the land ice (experiment OC) or the CO_2 concentration (experiment OI) is kept fixed at PI level. The synergy of land ice and CO_2 changes is negligibly small, meaning their induced temperature changes add approximately linearly when both forcings are applied. Likewise as in Stap et al. (2018), we use the simple energy balance model of Köhler et al. (2010) to analyse the applied radiative forcing of land ice albedo and CO_2 changes and simulated global temperature changes, after averaging to 1,000 year temporal resolution (Fig. 1a,b).

2.2.2 Proxy-inferred paleoclimate dataset

To compare our new approach for $S^{\varepsilon}_{[\mathrm{CO_2,LI}]}$ to our previous quantification of $S_{[\mathrm{CO_2,LI}]}$ (Köhler et al., 2018), we reanalyse the same paleoclimate dataset (introduced in Köhler et al., 2015), which contains reconstructions of ΔT_{g}, $\Delta R_{[\mathrm{CO_2}]}$, and $\Delta R_{[\mathrm{LI}]}$. Although this dataset covers the past 5 Myr, we focus on the past 800 kyr (Fig. 1c,d) because over this period $\Delta R_{[\mathrm{CO_2}]}$ is constrained by high-fidelity ice core CO_2 data, whereas Pliocene and Early Pleistocene CO_2 levels are still heavily debated (e.g. Badger et al., 2013; Martínez-Botí et al., 2015; Willeit et al., 2015; Stap et al., 2016, 2017; Chalk et al., 2017). Radiative forcing by CO_2 is obtained from Antarctic ice core data compiled by Bereiter et al. (2015), using $\Delta R_{[\mathrm{CO_2}]} = 5.35\,\mathrm{W\,m^{-2}} \cdot \ln(\mathrm{CO_2}/(278\,\mathrm{ppm}))$ (Myhre et al., 1998). Revised formulations of $\Delta R_{[\mathrm{CO_2}]}$ following Etminan et al. (2016) lead to very similar results with less than 0.01 $\mathrm{W\,m^{-2}}$ differences between the approaches for typical late Pleistocene CO_2 values (Köhler et al., 2017a). Radiative forcing caused by land ice albedo changes, as well as the global surface air temperature record (ΔT_{g}), are based on results of the 3D ice-sheet model ANICE (de Boer et al., 2014). ANICE was forced by northern hemispheric temperatures obtained from a benthic δ^{18}O stack (Lisiecki and Raymo, 2005) using an inverse technique. This provided geographically specific land ice distributions, and hence radiative forcing due to albedo changes with respect to PI on both hemispheres. In Köhler et al. (2015), the northern hemispheric (NH) temperature anomalies (ΔT_{NH}) are translated into global temperature perturbations using polar amplification factors ($f_{\mathrm{PA}} = \Delta T_{\mathrm{NH}}/\Delta T_{\mathrm{g}}$) as follows: at the LGM, $f_{\mathrm{PA}} = 2.7$ is taken from the average of PMIP3 model data (Braconnot et al., 2012), while at the mid-Pliocene Warm Period (mPWP, about 3.2 Myr ago), $f_{\mathrm{PA}} = 1.6$ is calculated from the average of PlioMIP results (Haywood et al., 2013). At all other times, f_{PA} is linearly varied as a function of NH temperature. The temperature dynamics follow from a benthic δ^{18}O stack and are unconstrained by climatic boundary conditions such as insolation and greenhouse gases, since ANICE only simulates land ice dynamics. Therefore, these results are here considered to be more similar to those of proxy-based reconstructions than of climate-model-based simulations. The temporal resolution of the dataset is 2,000 years.

Analysing this dataset, Köhler et al. (2018) found a temperature-CO_2 divergence appearing mainly during, or in connection with, periods of decreasing obliquity related to land ice growth or sea level fall. For these periods, a significantly different $S_{[\mathrm{CO2,LI}]}$ was obtained than for the remainder of the time frame. However, in the future we expect sea level to rise, hence these

Earth Syst. Dynam. Discuss., https://doi.org/10.5194/esd-2018-88
Manuscript under review for journal Earth Syst. Dynam.
Discussion started: 17 December 2018

Earth System Dynamics Discussions Open Access EGU

intervals of strong temperature-CO_2 divergence should not be considered for the interpretation of paleodata in the context of future warming, e.g. by using paleodata to constrain ECS. In the following analysis, we therefore exclude these times with strong temperature-CO_2 divergence, leaving 217 data points.

3 Results and Discussion

In this section, we will first demonstrate our new approach using a model-based dataset covering the past 5 Myr (Sect. 3.1), where the influence of land ice changes on the climate is a-priori known (Fig. 1a,b). Thereafter, we will apply it to a proxy-based reconstruction of paleoclimate of the past 800 kyr (Fig. 1c,d). We will base the efficacy of land ice changes on the relative influence this process has on the LGM temperature anomaly, as obtained from a range provided by a recent compilation (Shakun, 2017) (Sect. 3.2) and from analysing PMIP3 model results (Braconnot et al., 2012) (Sect. 3.3).

3.1 Demonstration of the approach using model simulations

CLIMBER-2 experiment OC, in which land ice is kept constant, approximately yields the sole effect of CO_2 changes on global temperature ($\Delta T_{[\mathrm{OC}]}$) since the influence of orbital variations is very small (Stap et al., 2018). We use a least-squares regression through scattered data of $\Delta R_{[\mathrm{CO_2}]}$ and $\Delta T_{[\mathrm{OC}]}$ to fit a second order polynomial (Fig. 2a). Using a higher order polynomial rather than a linear function allows us to capture state dependency of paleoclimate sensitivity. Fitting even higher order polynomials leads to negligible coefficients for the higher powers, and is not pursued further. From the fit, we calculate a specific paleoclimate sensitivity $S^{\varepsilon}_{[\mathrm{CO_2,LI}]}$ - in this case equal to $S^{\varepsilon}_{[\mathrm{CO_2}]}$ as there are no land ice changes - of 0.74 $\mathrm{K\,W^{-1}\,m^2}$ for PI conditions ($\Delta R_{[\mathrm{CO_2}]} = 0\ \mathrm{W\,m^{-2}}$) using Eq. 15. The fit further shows decreasing $S^{\varepsilon}_{[\mathrm{CO_2,LI}]}$ for rising $\Delta R_{[\mathrm{CO_2}]}$.

Our approach of compensating paleoclimate sensitivity for slow processes other than CO_2 changes, aims to deduce the same $S^{\varepsilon}_{[\mathrm{CO_2,LI}]}$ from experiment OIC in which both CO_2 and land ice cover vary over time as for experiment OC. First, we calculate the efficacy of land ice changes for the LGM from experiment OI, in which the CO_2 concentration is kept constant, and obtain $\omega = \Delta T_{[\mathrm{LI}]}/\Delta T_{\mathrm{g}} = \Delta T_{[\mathrm{OI}]}/\Delta T_{[\mathrm{OIC}]} = 0.54$. Consequently, we find $\varepsilon_{[\mathrm{LI}]} = 0.58$ from Eq. 11. Next, we calculate $\Delta T^{\varepsilon}_{[\mathrm{CO_2-equiv}]}$ using Eq. 13, and again fit a second order polynomial to the scattered data of $\Delta T^{\varepsilon}_{[\mathrm{CO_2-equiv}]}$ and $\Delta R_{[\mathrm{CO_2}]}$ (Fig. 2b). Between $\Delta R_{[\mathrm{CO_2}]} = -0.5\,\mathrm{W\,m^{-2}}$ and $\Delta R_{[\mathrm{CO_2}]} = 0.5\,\mathrm{W\,m^{-2}}$ there are some outlying values caused by division of small numbers. To remove these outliers, we first calculate the root mean square error (RMSE) between the fit and the data in the remainder of the domain. Then, we exclude all 144 values from the range $\Delta R_{[\mathrm{CO_2}]} = -0.5\,\mathrm{W\,m^{-2}}$ to $\Delta R_{[\mathrm{CO_2}]} = 0.5\,\mathrm{W\,m^{-2}}$ where the fit differs from the data by more than 3 $\times$ RMSE, and perform the regression again. This yields an $S^{\varepsilon}_{[\mathrm{CO_2,LI}]}$ of 0.72 $\mathrm{K\,W^{-1}\,m^2}$ for PI (Fig. 2b), which supports our approach since it is only slightly lower than the $S_{[\mathrm{CO_2,LI}]}$ of 0.74 $\mathrm{K\,W^{-1}\,m^2}$ obtained from experiment OC, which it should approximate. Here, the relationship between $\Delta T^{\varepsilon}_{[\mathrm{CO_2-equiv}]}$ and $\Delta R_{[\mathrm{CO_2}]}$ (Fig. 2b) is more linear than that of $\Delta T_{[\mathrm{OC}]}$ and $\Delta R_{[\mathrm{CO_2}]}$ (Fig. 2a) suggesting that the corresponding $S_{[\mathrm{CO_2,LI}]}$ increases more towards colder climates than in experiment OC, possibly indicating a non-constant $\varepsilon_{[\mathrm{LI}]}$. However, the difference between the $S^{\varepsilon}_{[\mathrm{CO_2,LI}]}$ obtained from both experiments remains smaller than 0.07 $\mathrm{K\,W^{-1}\,m^2}$ in the simulated domain. In

Earth Syst. Dynam. Discuss., https://doi.org/10.5194/esd-2018-88
Manuscript under review for journal Earth Syst. Dynam.
Discussion started: 17 December 2018

any case, the new approach considering efficacies clearly leads to a more satisfactory result than the old approach, which is equivalent to using $\varepsilon_{[\mathrm{LI}]} = 1$, and would give a PI $S_{[\mathrm{CO_2,LI}]}$ of $0.54\,\mathrm{K\,W^{-1}\,m^2}$ (Fig. 2c).

3.2 Application to proxy-inferred paleoclimate data

We proceed to apply our approach to a paleoclimate dataset inferred from proxies (Köhler et al., 2015). Other than for climate model simulations, the influence of land ice changes on global temperature perturbations cannot be directly obtained from proxy-based datasets, and is hence a-priori unknown. We therefore consider the study of Shakun (2017), who compiled this influence for the LGM using a 12-member climate model ensemble. He found a range of $46 \pm 14\%$ (mean $\pm 1\sigma$, full range $20 - 68\%$) for the simulated relative impact of land ice changes on the LGM temperature anomaly. Using these numbers in Eq. 11 yields $\varepsilon_{[\mathrm{LI}]} = 0.49^{+0.37}_{-0.22}$, from which we calculate $\Delta T^{\varepsilon}_{[\mathrm{CO_2-equiv}]}$ for the whole 800-kyr period. Fitting second order polynomials by least-squares regression to the scattered data of $\Delta T^{\varepsilon}_{[\mathrm{CO_2-equiv}]}$ and $\Delta R_{[\mathrm{CO_2}]}$ again, we infer a PI $S^{\varepsilon}_{[\mathrm{CO_2,LI}]}$ of $2.37^{+0.55}_{-0.56}\,\mathrm{K\,W^{-1}\,m^2}$ (Fig. 3a). The substantial uncertainty given here only reflects the 1σ uncertainty in $\varepsilon_{[\mathrm{LI}]}$. Similarly as before (Köhler et al., 2018), we detect a state dependency with decreasing $S^{\varepsilon}_{[\mathrm{CO_2,LI}]}$ towards colder climates for this dataset, more strongly so in case of lower $\varepsilon_{[\mathrm{LI}]}$. A discussion of this state-dependency of paleoclimate sensitivity, which is opposite to the one found in the previous section, is not followed any further here, but it has been analyzed in-depth in a previous publication (Köhler et al., 2018). At $\Delta R_{[\mathrm{CO_2}]} = 2.04\,\mathrm{W\,m^{-2}}$, the LGM value (here taken as the mean of 20 and 22 kyr ago), $S^{\varepsilon}_{[\mathrm{CO_2,LI}]}$ is only $1.39^{+0.35}_{-0.36}\,\mathrm{K\,W^{-1}\,m^2}$. The specific paleoclimate sensitivities we find here are generally higher than calculated by the old approach ($\varepsilon_{[\mathrm{LI}]} = 1$), which, for instance, for PI yields a $S_{[\mathrm{CO_2,LI}]}$ of $1.66\,\mathrm{K\,W^{-1}\,m^2}$ (Fig. 3b). This is because using this range for the impact of land ice changes on the LGM temperature anomaly, the efficacy factor $\varepsilon_{[\mathrm{LI}]}$ is smaller than unity. That means that these land ice changes contribute per unit radiative forcing comparatively less to the global temperature anomalies than the $\mathrm{CO_2}$ changes.

To compare our inferred $S^{\varepsilon}_{[\mathrm{CO_2,LI}]}$ to the ECS calculated by climate models, we scale them by a factor of 0.64 that accounts for the influence of other long-term processes, namely vegetation, aerosol and non-$\mathrm{CO_2}$ GHG changes (PALAEOSENS Project Members, 2012). Note that this scaling still assumes unit efficacy for all other processes than land ice changes. Therefore, it is a source of uncertainty to be investigated in future research. After multiplying by $3.7\,\mathrm{W^{-1}\,m^2}$, the radiative forcing perturbation representing a $\mathrm{CO_2}$ doubling (Myhre et al., 1998), we obtain an equivalent ECS of $5.6 \pm 1.3\,\mathrm{K}$ per $\mathrm{CO_2}$ doubling. This is on the high end of the results of other approaches to obtain ECS (Knutti et al., 2017), e.g. the 2.0 to 4.3 K 95%-confidence range from a large model ensemble (Goodwin et al., 2018), and the 2.2 to 3.4 K 66% confidence range from an emerging constraint from global temperature variability and CMIP5 (Cox et al., 2018). The efficacy of land ice changes has to be stronger (larger $\varepsilon_{[\mathrm{LI}]}$) than what we calculate so far from Shakun (2017) to achieve a smaller ECS and therefore a better agreement with these other estimates.

3.3 Further analysis of the influence of land ice changes on the LGM climate

In the previous section, we showed that the uncertain influence of land ice changes on the LGM temperature anomaly has a large effect on the calculated climate sensitivity. Here, we will make a complementary assessment of this influence of land ice

Earth Syst. Dynam. Discuss., https://doi.org/10.5194/esd-2018-88
Manuscript under review for journal Earth Syst. Dynam.
Discussion started: 17 December 2018

changes by analysing data from the PMIP3 model intercomparison project (Braconnot et al., 2012).

The PMIP3 ensemble consists of 9 general circulation models (Table 1). We investigate the intermodel relation between global average and northern high-latitude temperature changes at the LGM with respect to PI, caused by all long-term processes other than CO_2 changes. Taking this approach, we presume that these other processes, in particular land ice changes, lead to stronger polar amplification of temperature anomalies than CO_2 changes. For the temperature changes (ΔT_{g} and ΔT_{NH}) we use the PMIP3 data from the LGM runs from which we subtract the reference PI results. We use the 40° to 85° N mean to represent the northern high latitudes (NH), which is roughly the area where ice sheets grow. Currently, the PMIP3 simulation set does not comprise separate LGM runs using only CO_2 forcing. Therefore, we use the ECS values as published in Forster et al. (2013) and Haywood et al. (2013) to calculate the influence of CO_2 on temperature ($\Delta T_{[\mathrm{CO_2}]}$) for all PMIP3 models. By using the same equation as before for the CO_2 greenhouse gas radiative forcing (Myhre et al., 1998), we find that ratio of $\Delta R_{[\mathrm{CO_2}]}$ between LGM (185 ppm CO_2) and PI (280 ppm CO_2), and PI and $2 \times CO_2$ is $\ln(185/280)/\ln(2) = -0.6$ in the PMIP3 experiments. We correct the induced $\Delta T_{[\mathrm{CO_2}]}$ of all individual models for this ratio. In our analysis, we presume that the influence of CO_2 changes is spatially uniform as is approximately the case in the CLIMBER-2 simulations (Stap et al., 2018).

We regress a least-squares linear fit between $(\Delta T_{\mathrm{g}} - \Delta T_{[\mathrm{CO_2}]})$ and $(\Delta T_{\mathrm{NH}} - \Delta T_{[\mathrm{CO_2}]})$, providing us with a functional relation between these variables (Fig. 4). This relation is significant on the 95% level, but subject to large uncertainties. The RMSE between the data and the derived relation is 1.64 K (Fig. 4; cyan). This implies a substantial uncertainty of 29% in the influence of CO_2 on temperature, similar to the full range shown by the model ensemble in Shakun (2017). The relation is furthermore strongly dependent on the models CNRM-CM5 and GISS-E2-R that produce the smallest and the largest temperature anomalies respectively. Conversely, MIROC-ESM and MRI-CGCM3 constitute the largest outliers in the relation. Removing these models would nearly halve the RMSE between the data and the derived relation to 0.88 K. Lastly, relating the LGM temperature anomalies directly to the ECS obtained from $2 \times CO_2$ experiments is possibly problematic (Crucifix, 2006). Hence, confidence in the induced relation would be greatly increased if: i) more models participated in the PMIP intercomparison project, and ii) separate LGM runs using only CO_2 forcing were executed within this framework.

Notwithstanding these considerations, we will apply the relation between ΔT_{g}, ΔT_{NH}, and $\Delta T_{\mathrm{CO_2}}$ to our paleoclimate dataset (Sect. 2.2.2) (Köhler et al., 2015). In this dataset, the global average LGM temperature perturbation is -5.7 K. This is obtained from a northern high-latitude temperature perturbation of -15.5 K. However, this high-latitude anomaly represents the surface air temperature over the land masses only, for which the perturbation is $\sim 13\%$ stronger than for the whole region including the ocean, as deduced from the PMIP3 data. We therefore infer a mean perturbation of -13.8 K for the whole 40° to 85° N region. Applying the relation we found earlier to our dataset, we infer a $\Delta T_{[\mathrm{CO_2}]}$ of -1.3 K (Fig. 4; yellow star). This gives us an (assumed) relative influence of CO_2 on global temperature of 0.23 ($\Delta T_{[\mathrm{CO_2}]}/\Delta T_{\mathrm{g}} = -1.3\ \mathrm{K}/-5.7\ \mathrm{K}$). Next, we account for the influence of changes in non-CO_2 greenhouse gases, vegetation and aerosol changes by multiplying this influence by 1.57 (PALAEOSENS Project Members, 2012), leading to a total influence of 36%. The remaining 64% can be attributed to the influence of land ice changes. This is on the high side of the full 20 to 68% range shown in Shakun (2017), which would contradict the limited influence of land ice changes advocated by that same study based on analysis of Late Pliocene and Early

Earth Syst. Dynam. Discuss., https://doi.org/10.5194/esd-2018-88
Manuscript under review for journal Earth Syst. Dynam.
Discussion started: 17 December 2018

Earth System Dynamics Discussions Open Access EGU

Pleistocene data.

The comparatively large inferred influence of ice sheet changes in our dataset can be explained by the relatively strong northern hemispheric temperature perturbation (-15.5 K) in combination with the PMIP3 average polar amplification factor 2.7 (Sect. 2.2.2). Using a slightly lower factor of 2.6, $\Delta T_{[\mathrm{CO_2}]}$ would be -1.8 K, and the relative influence of ice sheet changes would decrease to 53%, which underlines the importance of correctly capturing polar amplification for constraining climate sensitivity. Using climate model output, the relative contributions of the land ice sheet change, $\mathrm{CO_2}$ change, and circulation on regional and global temperature can be calculated. For instance, Romanova et al. (2006) showed that changes in ice sheet height and ocean heat transport can significantly affect the tropical and high-latitude temperature response. A logical next step would be the analysis of the feedback mechanisms in a comprehensive model set-up, which is beyond the scope of the present paper.

Using Eq. 11 with the obtained $\omega = 0.64$ and the LGM values of our dataset, we calculate an $\varepsilon_{[\mathrm{LI}]}$ of 1.06. As $\varepsilon_{[\mathrm{LI}]} > 1$, the efficacy of land ice changes is larger than that of $\mathrm{CO_2}$ changes in this case. The corresponding PI $S^{\varepsilon}_{[\mathrm{CO_2,LI}]}$ is 1.61 $\mathrm{K\,W^{-1}\,m^2}$ (Fig. 3d), equivalent to an ECS of 3.8 K per $\mathrm{CO_2}$ doubling.

4 Conclusions

We have incorporated the concept of a time-constant efficacy factor (Hansen et al., 2005), that interrelates the global temperature responses to radiative forcing caused by land ice changes and $\mathrm{CO_2}$ changes, into our framework of calculating specific paleoclimate sensitivity $S^{\varepsilon}_{[\mathrm{CO_2,LI}]}$. The aim of this effort has been to overcome the problem that land ice and $\mathrm{CO_2}$ changes can lead to significantly different global temperature responses, even when they induce the same global-average radiative forcing. Firstly, we have shown the importance of considering efficacy differences by applying our new approach to results of 5-Myr CLIMBER-2 simulations (Stap et al., 2018), where the separate effects of land ice changes and $\mathrm{CO_2}$ changes can be isolated. In future research, the assumption that the efficacy factor is indeed constant in time could be tested more rigorously using more sophisticated climate models. Thereafter, we have used our new approach to reanalyse a 800-kyr proxy-inferred paleoclimate dataset (Köhler et al., 2015). We have implemented a range in the land ice change efficacy factor $\varepsilon_{[\mathrm{LI}]}$ based on the $46 \pm 14\%$ (mean $\pm 1\sigma$) impact of land ice changes on the LGM temperature anomaly simulated by a 12-member climate model ensemble (Shakun, 2017). We infer large uncertainty in the calculated PI $S^{\varepsilon}_{[\mathrm{CO_2,LI}]}$ of $2.37^{+0.55}_{-0.56}\,\mathrm{K\,W^{-1}\,m^2}$ caused by the implemented range in the efficacy factor $\varepsilon_{[\mathrm{CO_2,LI}]}$ which has a non-linear effect. The equivalent ECS corresponding to this $S^{\varepsilon}_{[\mathrm{CO_2,LI}]}$ is $5.6 \pm 1.3\,\mathrm{K}$ per $\mathrm{CO_2}$ doubling, only the lower end of which can be reconciled with estimates from other approaches. As this lower end tallies with higher values of $\varepsilon_{[\mathrm{CO_2,LI}]}$, our result suggests a large effect of land ice changes on global temperature anomalies. This finding is corroborated by a separate assessment of the influence of land ice changes on the LGM temperature anomaly and the corresponding efficacy $\varepsilon_{[\mathrm{CO_2,LI}]}$ based on PMIP3 data. Using this data, we have derived a functional relation between global and high-latitude temperature changes at the LGM with respect to the pre-industrial simulation (PI), and the temperature change caused by a change in $\mathrm{CO_2}$. By applying this relation to our proxy-inferred dataset, we have deduced a $\mathrm{CO_2}$-induced temperature change at LGM of -1.3 K. This result is, however, subject to substantial uncertainty stemming from

Earth Syst. Dynam. Discuss., https://doi.org/10.5194/esd-2018-88
Manuscript under review for journal Earth Syst. Dynam.
Discussion started: 17 December 2018

the derived functional relation and the polar amplification factor used in our dataset. Following from this CO_2-induced temperature change, the influence of land ice changes on the LGM temperature anomaly is 64%, even higher than the range used before but within the full 20 to 68% range shown in Shakun (2017). The associated PI $S^{\varepsilon}_{[CO_2,LI]}$ in this case is 1.61 $K\,W^{-1}\,m^2$, equivalent to an ECS of 3.8 K per CO_2 doubling.

Data availability. The CLIMBER-2 dataset is available at https://doi.pangaea.de/10.1594/PANGAEA.887427, and the proxy-inferred paleoclimate dataset is available at https://doi.pangaea.de/10.1594/PANGAEA.855449, from the PANGAEA database. For more information or data, please contact the authors.

Author contributions. L.B.S. designed the research. L.B.S. and P.K. performed the analysis. L.B.S. drafted the paper, with input from all co-authors.

Competing interests. The authors declare that they have no conflict of interest.

Acknowledgements. This work is institutional-funded at AWI via the research program PACES-II of the Helmholtz Association. We thank Roderik van de Wal for commenting on an earlier draft of the manuscript.

Earth Syst. Dynam. Discuss., https://doi.org/10.5194/esd-2018-88
Manuscript under review for journal Earth Syst. Dynam.
Discussion started: 17 December 2018

References

Badger, M. P. S., Lear, C. H., Pancost, R. D., Foster, G. L., Bailey, T. R., Leng, M. J., and Abels, H. A.: CO_2 drawdown following the middle Miocene expansion of the Antarctic Ice Sheet, Paleoceanography, 28, 42–53, 2013.

Bereiter, B., Eggleston, S., Schmitt, J., Nehrbass-Ahles, C., Stocker, T. F., Fischer, H., Kipfstuhl, S., and Chappellaz, J.: Revision of the EPICA Dome C CO_2 record from 800 to 600 kyr before present, Geophysical Research Letters, 42, 542–549, 2015.

Braconnot, P., Harrison, S. P., Kageyama, M., Bartlein, P. J., Masson-Delmotte, V., Abe-Ouchi, A., Otto-Bliesner, B., and Zhao, Y.: Evaluation of climate models using palaeoclimatic data, Nature Climate Change, 2, 417–424, 2012.

Brovkin, V., Ganopolski, A., and Svirezhev, Y.: A continuous climate-vegetation classification for use in climate-biosphere studies, Ecological Modelling, 101, 251–261, 1997.

Chalk, T. B., Hain, M. P., Foster, G. L., Rohling, E. J., Sexton, P. F., Badger, M. P. S., Cherry, S. G., Hasenfratz, A. P., Haug, G. H., Jaccard, S. L., et al.: Causes of ice age intensification across the Mid-Pleistocene Transition, Proceedings of the National Academy of Sciences, 114, 13 114–13 119, 2017.

Charney, J. G., Arakawa, A., Baker, D. J., Bolin, B., Dickinson, R. E., Goody, R. M., Leith, C. E., Stommel, H. M., and Wunsch, C. I.: Carbon dioxide and climate: a scientific assessment, National Academy of Sciences, Washington, DC, 1979.

Covey, C., Sloan, L. C., and Hoffert, M. I.: Paleoclimate data constraints on climate sensitivity: the paleocalibration method, Climatic Change, 32, 165–184, 1996.

Cox, P. M., Huntingford, C., and Williamson, M. S.: Emergent constraint on equilibrium climate sensitivity from global temperature variability, Nature, 553, 319, 2018.

Crucifix, M.: Does the Last Glacial Maximum constrain climate sensitivity?, Geophysical Research Letters, 33, 2006.

de Boer, B., van de Wal, R. S. W., Lourens, L. J., Bintanja, R., and Reerink, T. J.: A continuous simulation of global ice volume over the past 1 million years with 3-D ice-sheet models, Climate Dynamics, 41, 1365–1384, 2013.

de Boer, B., Lourens, L. J., and van de Wal, R. S. W.: Persistent 400,000-year variability of Antarctic ice volume and the carbon cycle is revealed throughout the Plio-Pleistocene, Nature Communications, 5, 2014.

Edwards, T. L., Crucifix, M., and Harrison, S. P.: Using the past to constrain the future: how the palaeorecord can improve estimates of global warming, Progress in Physical Geography, 31, 481–500, 2007.

Etminan, M., Myhre, G., Highwood, E. J., and Shine, K. P.: Radiative forcing of carbon dioxide, methane, and nitrous oxide: A significant revision of the methane radiative forcing, Geophysical Research Letters, 43, 2016.

Forster, P. M., Andrews, T., Good, P., Gregory, J. M., Jackson, L. S., and Zelinka, M.: Evaluating adjusted forcing and model spread for historical and future scenarios in the CMIP5 generation of climate models, Journal of Geophysical Research: Atmospheres, 118, 1139–1150, 2013.

Friedrich, T., Timmermann, A., Tigchelaar, M., Timm, O. E., and Ganopolski, A.: Non-linear climate sensitivity and its implications for future greenhouse warming, Science Advances, 2, e1501 923, 2016.

Ganopolski, A., Petoukhov, V., Rahmstorf, S., Brovkin, V., Claussen, M., Eliseev, A., and Kubatzki, C.: CLIMBER-2: a climate system model of intermediate complexity. Part II: model sensitivity, Climate Dynamics, 17, 735–751, 2001.

Goodwin, P., Katavouta, A., Roussenov, V. M., Foster, G. L., Rohling, E. J., and Williams, R. G.: Pathways to 1.5° C and 2° C warming based on observational and geological constraints, Nature Geoscience, p. 1, 2018.

Hansen, J., Sato, M. K. I., Ruedy, R., Nazarenko, L., Lacis, A., Schmidt, G. A., Russell, G., Aleinov, I., Bauer, M., Bauer, S., et al.: Efficacy of climate forcings, Journal of Geophysical Research: Atmospheres, 110, 2005.

Haywood, A. M., Hill, D. J., Dolan, A. M., Otto-Bliesner, B. L., Bragg, F., Chan, W.-L., Chandler, M. A., Contoux, C., Dowsett, H. J., Jost, A., et al.: Large-scale features of Pliocene climate: results from the Pliocene Model Intercomparison Project, Climate of the Past, 9, 191–209, 2013.

Knutti, R., Rugenstein, M. A. A., and Hegerl, G. C.: Beyond equilibrium climate sensitivity, Nature Geoscience, 10, 727, 2017.

Köhler, P., Bintanja, R., Fischer, H., Joos, F., Knutti, R., Lohmann, G., and Masson-Delmotte, V.: What caused Earth's temperature variations during the last 800,000 years? Data-based evidences on radiative forcing and constraints on climate sensitivity, Quaternary Science Reviews, 29, 129–145, https://doi.org/10.1016/j.quascirev.2009.09.026, 2010.

Köhler, P., de Boer, B., von der Heydt, A. S., Stap, L. B., and van de Wal, R. S. W.: On the state-dependency of the equilibrium climate sensitivity during the last 5 million years, Climate of the Past, 11, 1801–1823, 2015.

Köhler, P., Nehrbass-Ahles, C., Schmitt, J., Stocker, T. F., and Fischer, H.: A 156 kyr smoothed history of the atmospheric greenhouse gases CO_2, CH_4, and N_2O and their radiative forcing, Earth System Science Data, 9, 363–387, https://doi.org/10.5194/essd-9-363-2017, 2017a.

Köhler, P., Stap, L. B., von der Heydt, A. S., de Boer, B., van de Wal, R. S. W., and Bloch-Johnson, J.: A state-dependent quantification of climate sensitivity based on paleo data of the last 2.1 million years, Paleoceanography, 32, 1102–1114, https://doi.org/10.1002/2017PA003190, 2017PA003190, 2017b.

Köhler, P., Knorr, G., Stap, L. B., Ganopolski, A., de Boer, B., van de Wal, R. S. W., Barker, S., and Rüpke, L. H.: The effect of obliquity-driven changes on paleoclimate sensitivity during the late Pleistocene, Geophysical Research Letters, 45, 6661–6671, 2018.

Laskar, J., Robutel, P., Joutel, F., Gastineau, M., Correia, A. C. M., Levrard, B., et al.: A long-term numerical solution for the insolation quantities of the Earth, Astronomy & Astrophysics, 428, 261–285, 2004.

Lisiecki, L. E. and Raymo, M. E.: A Pliocene-Pleistocene stack of 57 globally distributed benthic δ^{18}O records, Paleoceanography, 20, 2005.

Martínez-Botí, M. A., Foster, G. L., Chalk, T. B., Rohling, E. J., Sexton, P. F., Lunt, D. J., Pancost, R. D., Badger, M. P. S., and Schmidt, D. N.: Plio-Pleistocene climate sensitivity evaluated using high-resolution CO_2 records, Nature, 518, 49–54, 2015.

Myhre, G., Highwood, E. J., Shine, K. P., and Stordal, F.: New estimates of radiative forcing due to well mixed greenhouse gases, Geophysical Research Letters, 25, 2715–2718, 1998.

PALAEOSENS Project Members: Making sense of palaeoclimate sensitivity, Nature, 491, 683–691, 2012.

Petoukhov, V., Ganopolski, A., Brovkin, V., Claussen, M., Eliseev, A., Kubatzki, C., and Rahmstorf, S.: CLIMBER-2: a climate system model of intermediate complexity. Part I: model description and performance for present climate, Climate Dynamics, 16, 1–17, 2000.

Romanova, V., Lohmann, G., Grosfeld, K., and Butzin, M.: The relative role of oceanic heat transport and orography on glacial climate, Quaternary Science Reviews, 25, 832–845, 2006.

Shakun, J. D.: Modest global-scale cooling despite extensive early Pleistocene ice sheets, Quaternary Science Reviews, 165, 25–30, 2017.

Stap, L. B., de Boer, B., Ziegler, M., Bintanja, R., Lourens, L. J., and van de Wal, R. S. W.: CO_2 over the past 5 million years: Continuous simulation and new δ^{11}B-based proxy data, Earth and Planetary Science Letters, 439, 1–10, 2016.

Stap, L. B., van de Wal, R. S. W., de Boer, B., Bintanja, R., and Lourens, L. J.: The influence of ice sheets on temperature during the past 38 million years inferred from a one-dimensional ice sheet–climate model, Climate of the Past, 13, 1243–1257, 2017.

Stap, L. B., Van de Wal, R. S. W., de Boer, B., Köhler, P., Hoencamp, J. H., Lohmann, G., Tuenter, E., and Lourens, L. J.: Modeled influence of land ice and CO_2 on polar amplification and paleoclimate sensitivity during the past 5 million years, Paleoceanography and Paleoclimatology, 33, 381–394, 2018.

Stocker, T. F., Mysak, L. A., and Wright, D. G.: A zonally averaged, coupled ocean-atmosphere model for paleoclimate studies, Journal of Climate, 5, 773–797, 1992.

Stuber, N., Ponater, M., and Sausen, R.: Why radiative forcing might fail as a predictor of climate change, Climate Dynamics, 24, 497–510, 2005.

van de Wal, R. S. W., de Boer, B., Lourens, L. J., Köhler, P., and Bintanja, R.: Reconstruction of a continuous high-resolution CO_2 record over the past 20 million years, Climate of the Past, 7, 1459–1469, https://doi.org/10.5194/cp-7-1459-2011, 2011.

Vial, J., Dufresne, J.-L., and Bony, S.: On the interpretation of inter-model spread in CMIP5 climate sensitivity estimates, Climate Dynamics, 41, 3339–3362, 2013.

von der Heydt, A. S., Köhler, P., van de Wal, R. S. W., and Dijkstra, H. A.: On the state dependency of fast feedback processes in (paleo) climate sensitivity, Geophysical Research Letters, 41, 6484–6492, 2014.

von der Heydt, A. S., Dijkstra, H. A., van de Wal, R. S. W., Caballero, R., Crucifix, M., Foster, G. L., Huber, M., Köhler, P., Rohling, E., Valdes, P. J., et al.: Lessons on climate sensitivity from past climate changes, Current Climate Change Reports, 2, 148–158, 2016.

Willeit, M., Ganopolski, A., Calov, R., Robinson, A., and Maslin, M.: The role of CO_2 decline for the onset of Northern Hemisphere glaciation, Quaternary Science Reviews, 119, 22–34, 2015.

Yoshimori, M., Hargreaves, J. C., Annan, J. D., Yokohata, T., and Abe-Ouchi, A.: Dependency of feedbacks on forcing and climate state in physics parameter ensembles, Journal of Climate, 24, 6440–6455, 2011.

Earth Syst. Dynam. Discuss., https://doi.org/10.5194/esd-2018-88
Manuscript under review for journal Earth Syst. Dynam.
Discussion started: 17 December 2018

Earth System Dynamics
Discussions
Open Access
EGU

Table 1. The PMIP3 models used here, along with their published equilibrium climate sensitivity (ECS), the LGM temperature anomaly caused only by CO_2 changes ($\Delta T_{[CO_2]}$) inferred from the ECS, and the global and northern hemispheric (40-85° N) temperature anomalies at the LGM with respect to their PI reference (ΔT_g, ΔT_{NH}).

Model	published ECS (K per CO_2-doubling)	Inferred LGM $\Delta T_{[CO_2]}$ (K)	LGM ΔT_g (K)	LGM ΔT_{NH} (K)
CCSM	2.9	-1.82	-4.91	-11.2
CNRM-CM5	3.3	-2.07	-2.62	-6.29
COSMOS-ASO	4.1	-2.58	-5.46	-11.2
FGOALS-g2	4.2	-2.64	-4.73	-11.6
GISS-E2-R	2.1	-1.32	-5.07	-14.0
IPSL-CM5A-LR	4.1	-2.58	-4.60	-10.0
MIROC-ESM	4.7	-2.95	-5.00	-14.4
MPI-ESM-P	3.5	-2.20	-4.41	-10.4
MRI-GCSM3	2.6	-1.63	-4.68	-8.89

Earth Syst. Dynam. Discuss., https://doi.org/10.5194/esd-2018-88
Manuscript under review for journal Earth Syst. Dynam.
Discussion started: 17 December 2018

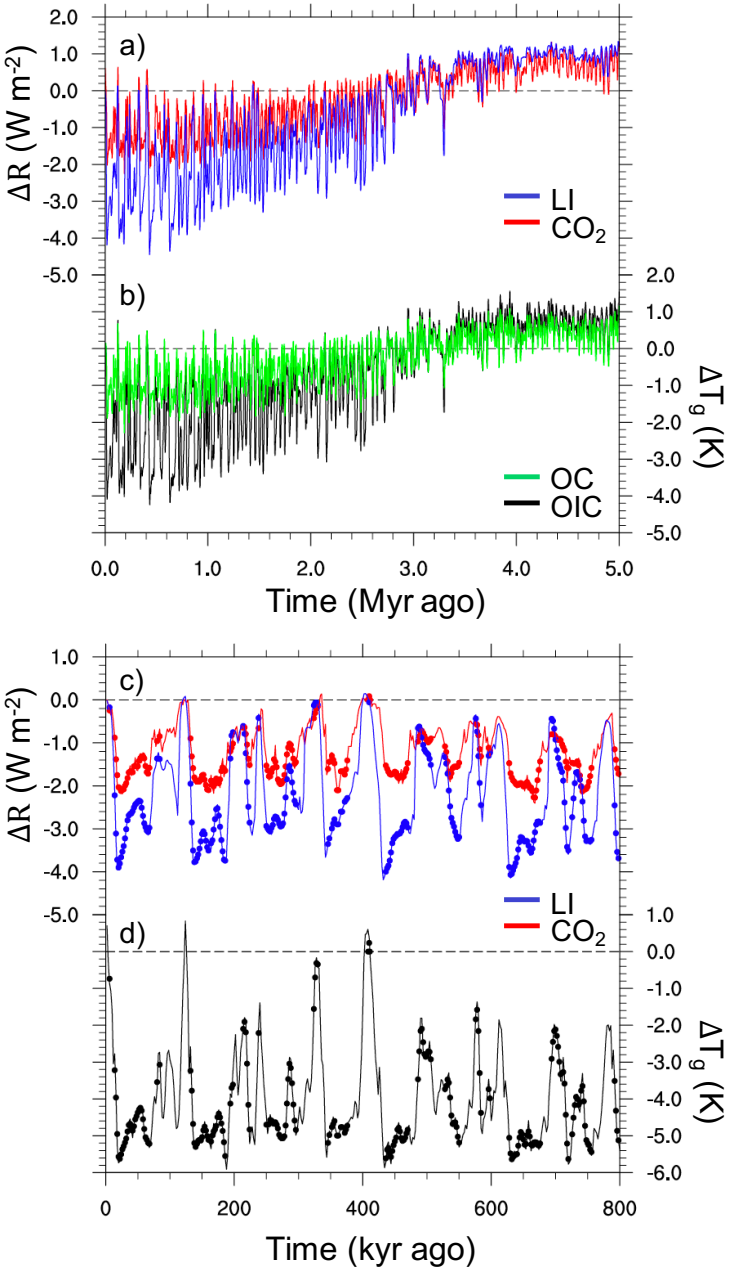

Figure 1. Timeseries of radiative forcing anomalies (ΔR) caused by CO_2 (red) changes and land ice changes (blue), and global temperature anomalies (ΔT_g) with respect to PI, from **a-b)** the CLIMBER-2 model dataset (Stap et al., 2018), with temperature data for experiment OIC in black and for experiment OC in green, and from **c-d)** the proxy-inferred dataset (Köhler et al., 2015), with solid lines for the whole dataset, and dots for the data used in this study which exclude times with strong temperature-CO_2 divergence (see Sect. 2.2.2). Note the differing axis scales.

Earth Syst. Dynam. Discuss., https://doi.org/10.5194/esd-2018-88
Manuscript under review for journal Earth Syst. Dynam.
Discussion started: 17 December 2018

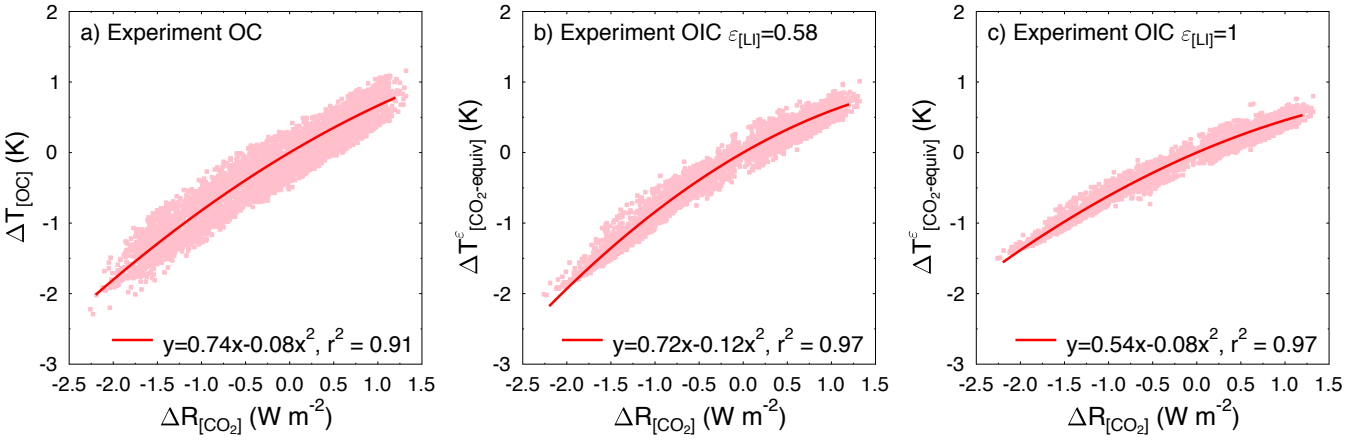

Figure 2. Temperature anomalies with respect to PI over the last 5 Myr from CLIMBER-2 (Stap et al., 2018) against imposed radiative forcing of CO_2. **a)** Simulation with fixed PI land ice distribution (experiment OC) ($\Delta T_{[\mathrm{OC}]}$). **b)** Calculated CO_2-equivalent temperature perturbations ($\Delta T^{\varepsilon}_{[\mathrm{CO_2-equiv}]}$) from experiment OIC using Eq. 13 with $\varepsilon_{[\mathrm{LI}]} = 0.58$. **c)** Same as in (b), but with $\varepsilon_{[\mathrm{LI}]} = 1$, which is equivalent to the old approach where efficacy differences were not considered. The red lines represent second order polynomial least-squares regressions through the scattered data.

Earth Syst. Dynam. Discuss., https://doi.org/10.5194/esd-2018-88
Manuscript under review for journal Earth Syst. Dynam.
Discussion started: 17 December 2018

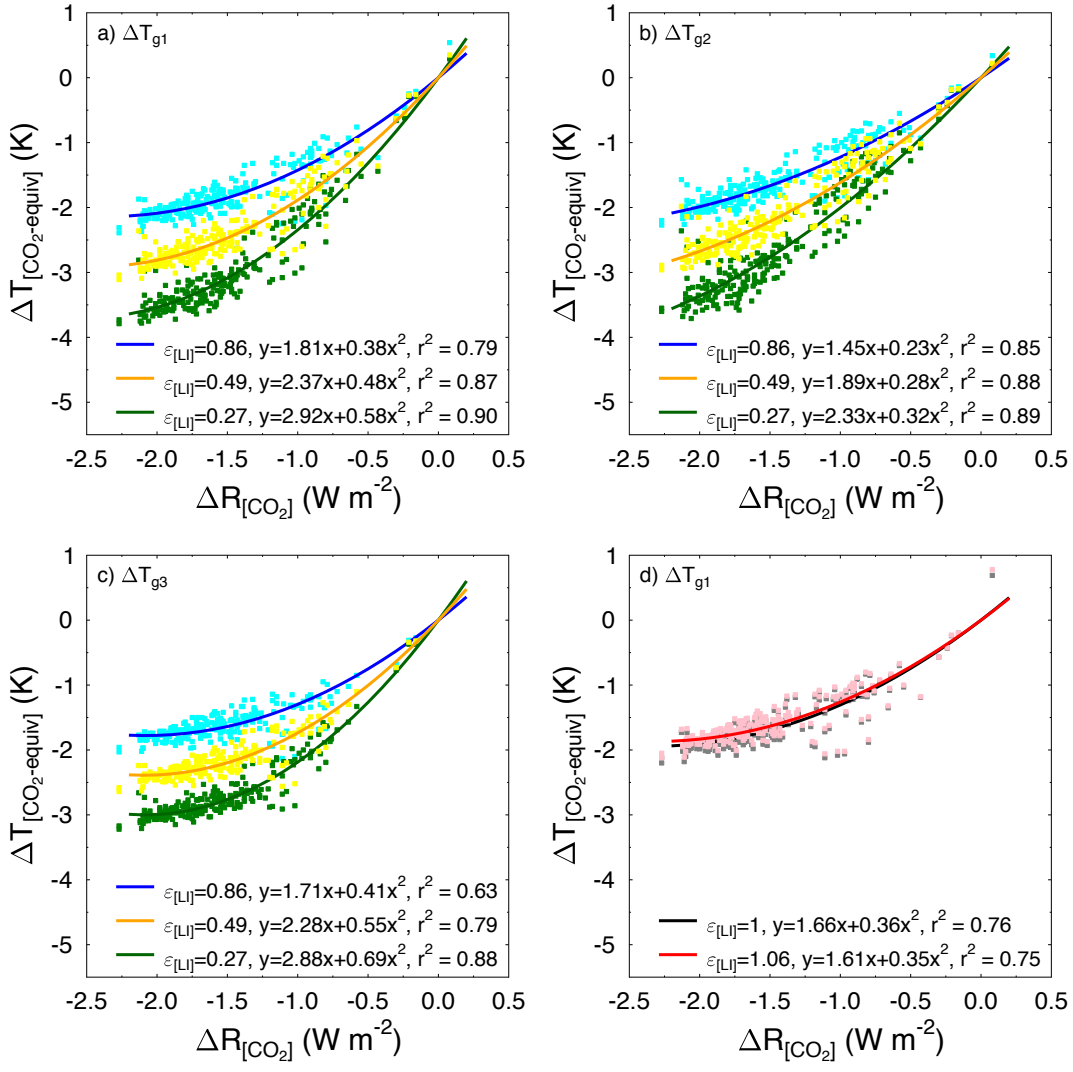

Figure 3. The CO_2-equivalent temperature perturbations ($\Delta T^{\varepsilon}_{[\mathrm{CO_2-equiv}]}$) calculated using Eq. 13 against $\Delta R_{[\mathrm{CO_2}]}$ from the proxy-inferred paleoclimate dataset (Köhler et al., 2015), using: **a)** $\varepsilon_{[\mathrm{LI}]} = 0.86$ (maroon dots), $\varepsilon_{[\mathrm{LI}]} = 0.49$ (cyan dots), and $\varepsilon_{[\mathrm{LI}]} = 0.27$ (green dots), and **b)** $\varepsilon_{[\mathrm{LI}]} = 1$ (grey dots), which is equivalent to the old approach, and $\varepsilon_{[\mathrm{LI}]} = 1.06$ (yellow dots). The brown, blue, dark green (**a**), black and orange lines (**b**) represent second order polynomial least-squares regressions through the data.

Earth Syst. Dynam. Discuss., https://doi.org/10.5194/esd-2018-88
Manuscript under review for journal Earth Syst. Dynam.
Discussion started: 17 December 2018

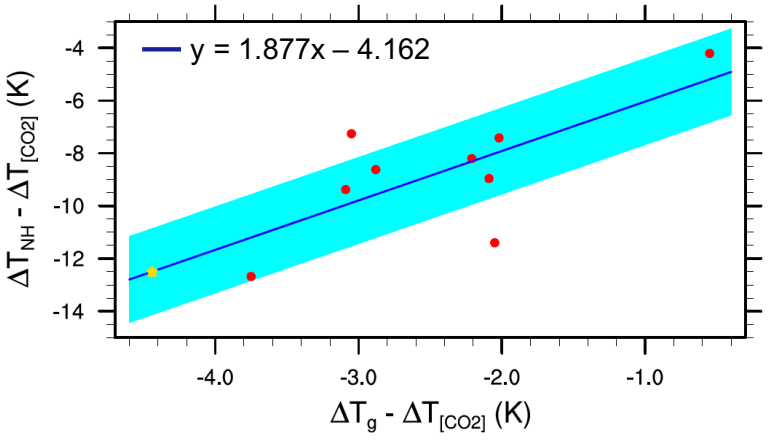

Figure 4. The Northern Hemisphere LGM temperature anomaly (ΔT_{NH}) minus the temperature anomaly caused only by CO_2 changes ($\Delta T_{[\mathrm{CO_2}]}$) inferred from the ECS, against the global LGM temperature anomaly (ΔT_{g}) minus $\Delta T_{[\mathrm{CO_2}]}$, for the models in the PMIP3 ensemble (red dots). The blue line is the regressed linear intermodel relation between these quantities. In cyan, the 1.64 K uncertainty determined from the root mean square difference between the data and the fit. The yellow star represents the values for ΔT_{NH}, ΔT_{g}, and $\Delta T_{[\mathrm{CO_2}]}$ deduced by applying the fit to the proxy-inferred paleoclimate dataset (Köhler et al., 2015), hence by construction being on the fitted line.